A New Brain Endocast of *Homo erectus* From Hulu Cave, Nanjing, China

Xiujie Wu,[1,2]* Ralph L. Holloway,[3] Lynne A. Schepartz,[4] and Song Xing[1,5]

[1]*Key Laboratory of Evolutionary Systematics of Vertebrates, Institute of Vertebrate Paleontology and Paleoanthropology, Chinese Academy of Sciences, Beijing 100044, China*
[2]*State Key Laboratory of Palaeobiology and Stratigraphy, Nanjing Institute of Geology and Palaeontology, Nanjing 210008, China*
[3]*Department of Anthropology, Columbia University, NY, NY 100027*
[4]*Department of Anthropology, Florida State University, Tallahassee, FL 32306-7772*
[5]*Graduate School of the Chinese Academy of Sciences, Beijing 100049, China*

KEY WORDS endocast; *Homo erectus*; Nanjing 1; brain evolution

ABSTRACT A new brain endocast of *Homo erectus* from Hulu Cave, Tangshan, Nanjing is described and compared with a broad sample of endocasts of *H. erectus*, Neanderthals, and recent modern humans. The Nanjing 1 endocast is reconstructed based on two portions of endocranial casts taken from the original fossil fragments. The fossil was discovered in 1993, near Nanjing, South China and is dated to ~ 0.58–0.62 Ma. The cranial capacity is ~ 876 cc, as determined by endocast water displacement. There are some common features of Nanjing 1 and other *H. erectus* endocasts that differentiate them from the Neanderthals and modern humans in our sample. These include small cranial capacity, low height dimensions, simple middle meningeal vessel patterns, a high degree of cerebral-over-cerebellar lobe overhang, elongated and quite separated cerebellar lobes, and a narrow, low, short and flat frontal region. Some features are found to vary among *H. erectus*, Neanderthals and modern humans, such as the lateral Sylvian fissure position and the venous sinus and petalial patterns. The Nanjing 1 endocast has unique, large, superior frontal convolutions, and strongly protruding Broca's caps. In contrast to other Chinese *H. erectus* from Hexian and Zhoukoudian, Nanjing 1 lacks strong posterior projection of the occipital lobes. Bivariate and principal component analyses indicate that the small volume and shape of Nanjing 1 is most similar to KNM-WT 15000, KNM-ER 3883, Sangiran 2 and Hexian, illustrating the combination of narrow, low, and short frontal lobes with wide posterior lobes. Am J Phys Anthropol 145:452–460, 2011.

Endocasts are the most direct evidence for studying human brain evolution. Endocasts can provide information on brain size, general shape, morphology, and anatomical features of the external surface. Over the past 100 plus years, since the endocast of *Pithecanthropus erectus* was manually reconstructed, a number of other hominin endocasts have been made including many of *Homo erectus* (e.g., Black, 1933; Dubois, 1933; Weidenreich, 1936, 1939; Holloway, 1980, 1981; Begun and Walker, 1993; Grimaud-Hervé, 1997; Broadfield et al., 2001; Holloway et al., 2004; Balzeau et al., 2005; Bruner and Manz, 2005; Wu et al., 2006, 2010). Several studies demonstrate that *H. erectus* specimens have different morphological features from Neanderthals and modern humans; these include small brain size, low position of the greatest breadth, low maximum height, narrow and relatively flat surfaces of the frontal lobes, a high degree of cerebral-over-cerebellar lobe overhang, elongated and quite separated cerebellar lobes, and relative simplicity of the meningeal vessels (Falk, 1993; Bruner, 2003; Grimaud-Hervé, 2004; Weaver, 2005). In light of these paleoneurological studies, the taxonomic affinity of Chinese *H. erectus* has been subject to question. For example, Begun and Walker (1993) suggested that the morphology of the Zhoukoudian (ZKD) *H. erectus* endocasts is similar, in its major features, to that of KNM-WT 15000. However, they also found that the ZKD endocasts possess unique morphological features that are not shared by the African and other Asian samples, such as a well-marked frontal keel—the prominent sagittal elevation running along the frontal and parietal lobes. Broadfield et al. (2001) found that the endocast of Sambungmacan 3 from Indonesia has a mosaic of features that are shared with both other Indonesian, and also ZKD, *H. erectus*. Wu et al. (2006), in their comparison of Hexian with ZKD, Sambungmacan 3 and KNM-WT 15000, found that Hexian from central-eastern China is morphologically more similar to the majority of the ZKD specimens. In the present study, we analyze a new reconstruction of the Nanjing 1 endocast. We compare

Grant sponsor: National Natural Science Foundation of China; Grant numbers: 40972017. Grant sponsor: International Cooperation Program of MST of China; Grant numbers: 2009DFB20580. Grant sponsor: State Key Laboratory of Palaeobiology and Stratigraphy of Nanjing Institute of Geology and Paleontology; Grant numbers: 093109. Grant sponsor: Chinese Academy of Sciences; Grant number: XDA05130101.

*Correspondence to: Xiujie Wu, Institute of Vertebrate Paleontology and Paleoanthropology, Chinese Academy of Sciences, Beijing 100044, China. E-mail: wuxiujie@ivpp.ac.cn

Received 25 October 2010; accepted 9 February 2011

DOI 10.1002/ajpa.21527
Published online 3 May 2011 in Wiley Online Library (wileyonlinelibrary.com).

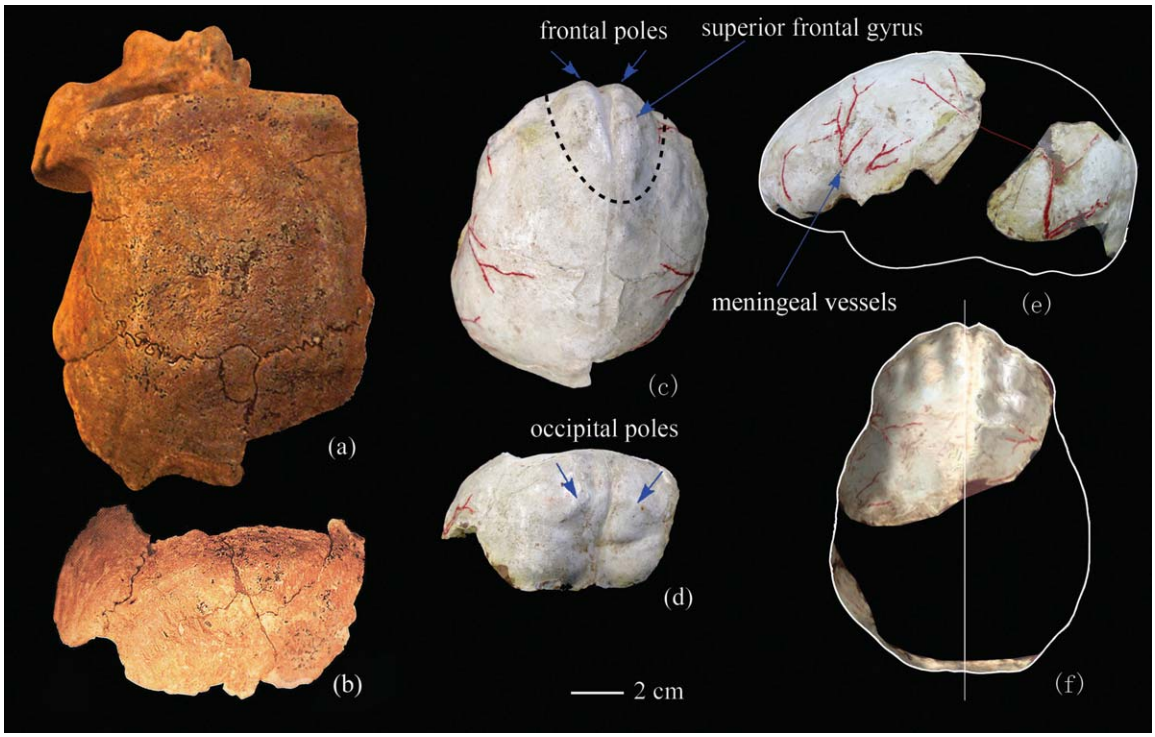

Fig. 1. The Nanjing 1 fragments and endocranial cast. (**a**) and (**c**) Anterior part of the cranial cap and the corresponding endocast portion; (**b**) and (**d**) Left parietal bone and the inferior occipital squama and the corresponding endocast portion; (**e**) Lateral view of the endocast portions showing the missing part and the position of the represented meningeal vessels in red; (**f**) Superior view of the endocast portions showing the right side of the cerebral hemisphere that is reconstructed for this study. In this view the endocast is positioned as it was for measurement, with the axis of the frontal and occipital poles parallel to a flat surface.

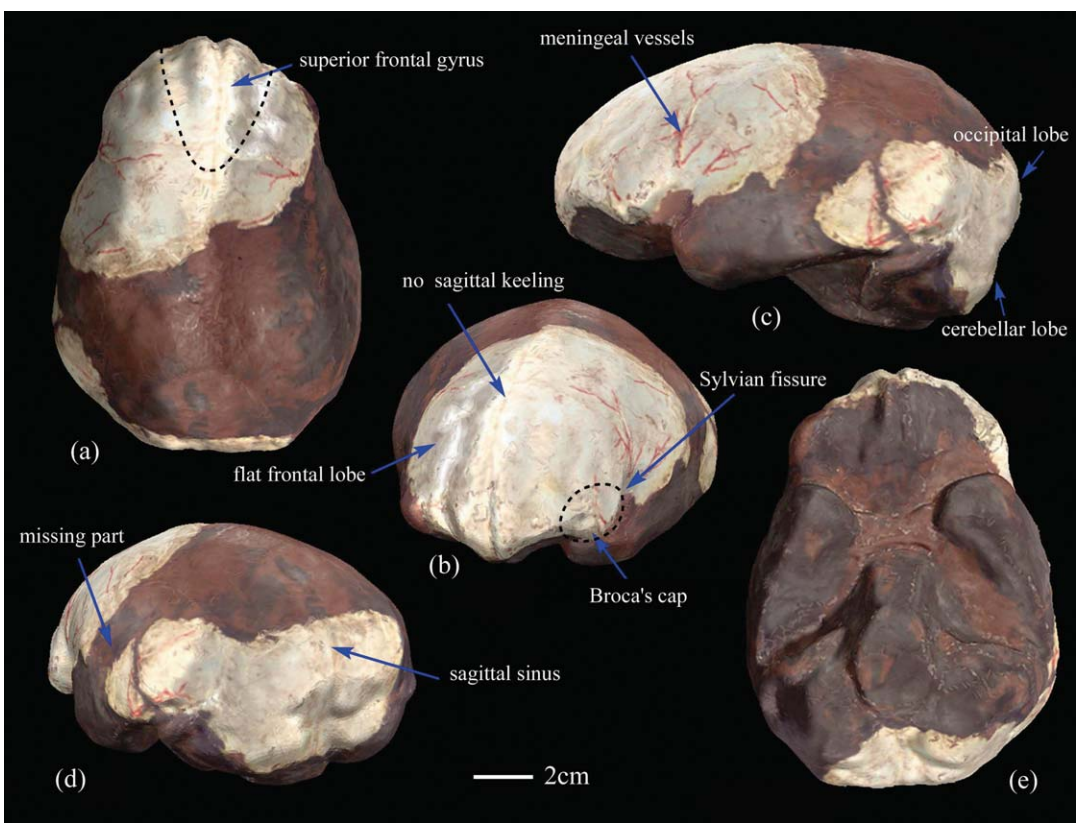

Fig. 2. Reconstruction of Nanjing 1 endocast. (**a**) Superior view; (**b**) Left anterior view; (**c**) Right lateral view; (**d**) Left posterior view; (**e**) Basal view.

its morphology with other *H. erectus*, Neanderthals, and modern humans in order to facilitate a more comprehensive understanding of the Nanjing 1 *H. erectus* brain morphology and to re-examine the variability of *H. erectus*.

THE NANJING 1 HUMAN FOSSIL

The Nanjing 1 remains were discovered in 1993 at the Hulu Cave near the Tangshan town of Nanjing in southern China (Tangshan Archaeological Excavation Team, 1996). Cranial morphological studies demonstrate that it shares a suite of features described as characteristic of *H. erectus* with both Eurasian and African specimens considered to be *H. erectus* (a low position for the maximum vault breadth, thick cranial bones, strong development of the torus supraorbitalis and torus angularis, and a well-developed torus occipitalis), and that it should be referred to that taxon (Liu et al., 2005).

The age of Nanjing 1 was initially suggested to be ~0.35 Ma according to ESR and U-series dating (Chen et al., 1997). Newer thermal ionization mass spectrometry U-series dating results suggest that the Nanjing hominin remains are older than 0.5 Ma (Zhou et al., 1999) and probably date to 0.58–0.62 Ma (Zhao et al., 2001). These new age estimates imply that Nanjing 1 is contemporaneous with the ZKD *H. erectus* specimens that have an age of 0.4–0.8 Ma (Shen et al., 2009). Geographically, the Nanjing or Huludong site lies between ZKD in North China and the more southern *H. erectus* localities of Indonesia.

When it was found, Nanjing 1 was in three pieces. The biggest fragment includes the frontal, one-third of the anterior part of the left parietal, a portion of the sphenoid, the nasal bones, and the left maxillary zygomatic bones (Fig. 1a); the second fragment consists of part of the occipital and the posterior portion of the left parietal (Fig. 1b); and the third fragment is a small piece of right parietal. An ectocranial lesion on the external frontal and parietals is exhibited, while the endocranial surfaces in the lesion are normal (Shang and Trinkaus, 2008). Using these fragments, a reconstructed of the cranium was made in 2002 (Wu et al., 2002; Zhang and Liu, 2002). The cranial capacity was estimated to be ~871 cc using Ding's formulae based on auricular height (Zhang and Liu, 2003). Two endocast portions of Nanjing 1 (Fig. 1c,d) were made by Zhang Yinyun based on the endocranial surfaces of the original cranial fragments; however, the Nanjing 1 endocast was not reconstructed completely and there were no publications on it.

RECONSTRUCTION OF NANJING 1 ENDOCAST

The Nanjing 1 endocast reconstruction included in this study is based on two endocranial casts from the original cranial fragments. One portion includes an almost complete frontal lobe, one-third of the anterior part of the left parietal lobe along with a small portion of the temporal lobe, and part of the right parietal lobe (Fig. 1c). The other portion consists of a partial left parietal and temporal lobe, the lower part of the occipital lobe, and most of the cerebellar lobes (Fig. 1d). The frontal bec, brain stem, foramen magnum, and most of the temporal and right parietal lobes were missing from the original, and thus had to be reconstructed, along with the upper cerebellar portion and a small inferior portion of the right cerebellar lobe.

The new reconstruction, using a light brown plasticine between the missing portions, was created following the curvatures provided by the extant portions of the frontal, parietal, occipital, and cerebellar lobes. Both cast portions contain part of the left parietal and temporal lobes, and the two frontal and occipital poles are preserved on the two original portions (Fig. 1c,d). Although there is a gap between the two pieces of left parietal, judging from the position of the meningeal vessels, the parietal and temporal lobe contours of the two pieces, the position of bregma and the preservation of the frontal and occipital poles that can be used to orient the casts along a sagittal axis, we created the missing part of the left cerebral hemisphere (Fig. 1e).

We then relied on symmetry to reconstruct the right side of the cerebral hemisphere (Fig. 1f). In addition, we used the six Zhoukoudian endocasts as guides in making our reconstruction. This method of reconstruction cannot be wholly without errors (Holloway et al., 2004), but it is based upon the expertise and experience RLH has gained through making similar reconstructions over the decades, even with CT virtual reconstruction, one still have to follow existing anatomical contours (e.g., Zollikofer and Ponce de Leon, 2005), and hopefully this will be attempted in the future. For the present, we believe this reconstruction offers an excellent approximation to the complete original.

After completion of the reconstruction of the basal portion (see Fig. 2), the volume was measured by water displacement. This yielded an average volume of ca. 876 cc from three readings ranging between 874 and 879 cc. The new volume determination is quite similar to the estimate of 871 cc from the first reconstruction (Zhang and Liu, 2003).

MATERIALS AND METHODS

Comparative samples

Sixty-four endocasts representative of *H. erectus* (n = 20), Neanderthals (n = 6), and recent modern humans (n = 38) were selected for comparisons with Nanjing 1 (Table 1). The selection of specimens was based on the need for endocasts with most of the frontal and occipital lobes intact—corresponding to the representation of the Nanjing 1 endocast. Nanjing 1, ZKD specimens III, II, X, XI, XII, and V, Hexian, Sambungmacan 3, and four European recent modern human endocasts are from the Institute of Vertebrate Paleontology and Paleoanthropology, Chinese Academy of Sciences; Trinil II, Sangiran 2 and 17, Ngandong 1, 6, 7 and 14, KNM-ER 3733 and 3883, KNM-WT 15000, OH 9, Salé, La Ferrassie, La Chapelle-aux-Saints, Spy 1 and 2, Guattari I, Forbes' Quarry, and 34 recent modern humans are from RLH's collection at Columbia University.

Morphometric methods

Metric data were collected on laser scanned virtual reconstructions of the endocasts using a NextEngine Model 2020i Desktop 3D Scanner (www.NextEngine.com) and Rapidworks™ software. The digitizer-based and 3D model-based coordinate measurements had overall standard deviations of, respectively, ±0.79 and ±1.05 mm, yielding the most precise coordinate data for landmarks defined primarily by biological criteria

TABLE 1. Materials used for comparisons with the Nanjing 1 endocast (n = 64)

	Specimen	Age (Ma)	Cranial capacity (cc)	References
H. erectus	ZKD II	0.68–0.78	1,020	Weidenreich, 1943; Shen et al., 2009
	ZKD III	0.68–0.78	915	Weidenreich, 1943; Shen et al., 2009
	ZKD V	0.40	1,140	Qiu et al., 1973; Shen et al., 2009
	ZKD X	0.68–0.78	1,225	Weidenreich, 1943; Shen et al., 2009
	ZKD XI	0.68–0.78	1,015	Weidenreich, 1943; Shen et al., 2009
	ZKD XII	0.68–0.78	1,030	Weidenreich, 1943; Shen et al., 2009
	Hexian	0.41	1,025	Wu and Dong, 1982; Grün et al., 1998
	Trinil II	0.7–1.0	940	Holloway, 1981; Swisher et al., 1994
	Sm 3	0.90	917	Broadfield et al., 2001; Delson et al., 2001
	Sg 2	0.7–1.6	815	Holloway, 1981; Swisher et al.,1994
	Sg 17	0.70	1,004	Holloway, 1981; Swisher et al.,1994
	Ng 1	0.031	1,172	Holloway, 1981; Swisher et al.,1994
	Ng 6	0.031	1,250	Holloway, 1981; Swisher et al.,1994
	Ng 7	0.031	1,013	Holloway, 1981; Swisher et al.,1994
	Ng 14	0.031	1,090	Holloway, 1981; Swisher et al.,1994
	3733	1.75	848	Holloway, 1981; Brown et al., 1985
	3883	1.4–1.6	804	Holloway, 1981; Brown et al., 1985
	15000	1.4–1.6	900	Begun and Walker, 1993; Brown and McDougall, 1993
	OH 9	1.50	1,067	Holloway, 1981; Brown et al., 1985
	Salé	0.40	880	Holloway, 1981; Brown et al., 1985
Neanderthals	LF	0.07	1,640	Holloway, 2004
	LC	0.06	1,625	Holloway, 2004
	Spy 1	0.068	1,305	Holloway, 2004
	Spy 2	0.068	1,553	Holloway, 2004
	Gt	0.04–0.06	1,360	Holloway, 2004
	FQ	0.05	1,200	Holloway, 2004
Modern humans (n = 36)	Recent	1,208–1,750		

Specimen name abbreviations: Zkoukoudian (ZKD), Sambungmacan (Sm), Sangiran (Sg), Ngandong (Ng), KNM-ER 3733 (3733), KNM-ER 3883 (3883), KNM-WT 15000 (15000), La Ferrassie (LF), La Chapelle-aux-Saints (LC), Guattari I (Gt), Forbes' Quarry (FQ).

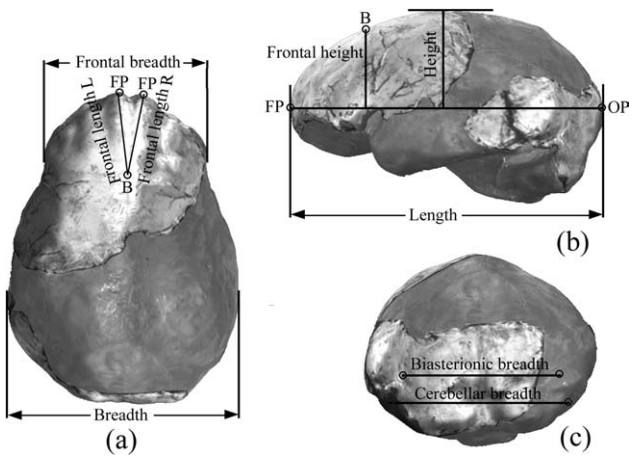

Fig. 3. Superior (**a**) left lateral (**b**), and posterior views (**c**) of Nanjing 1 virtual endocast showing the landmarks for the metric variables. FP: frontal pole, OP: occipital pole, B: bregma, Length: maximum projection chord length between the frontal and occipital poles, Breadth: maximum projection width at the temporo-parietal surface, Frontal breadth: maximum projection width on the triangular part of third frontal gyrus, Frontal length: B-FP, Frontal height: the projection height from B to the line of FP-OP, Height: the projection height from the vault top to the line of FP-OP, Biasterionic breadth: biasterionic projection breadth, Cerebellar breadth: maximum projection width of the occipital lobes perpendicular to the sagittal plane, excluding the sigmoid sinuses.

(Sholts et al., 2010). To standardize the measuring procedure, each endocast was placed on a flat surface with the horizontal plane along the axis of the frontal and occipital poles (left side) parallel to the flat surface. The specimen remained with the axis of the frontal and occipital poles parallel to the flat surface whether rotated for a superior or lateral view. According to the preserved aspects of the Nanjing 1 specimen, we choose nine standardized measurements (see detail in Fig. 3). These are length (the greater of the two hemisphere lengths), breadth (the greater of the two hemisphere lengths perpendicular to the sagittal plane), frontal breadth (the maximum projection width on the triangular part of the third frontal gyrus), frontal length L (the left maximum chord from bregma to the left frontal pole), frontal length R (the right maximum chord from bregma to the right frontal pole), frontal height (the projection height from bregma to the line of FP-OP), height (the projection height from the vault top to the line of FP-OP), biasterionic breadth (the biasterionic projection breadth), and cerebellar breadth (the maximum projection width of the occipital lobes perpendicular to the sagittal plane excluding the sigmoid sinuses). Each endocast was measured three times and the average was used as the final measurement.

Statistical analyses were performed using SPSS (13.0). Bivariate plots and principal component analyses (PCA) were used to examine the interactions among variables. As some of the measurements (e.g., length) are highly dependent on our reconstruction whereas others are not, we choose the more reliable measurements for the morphometric analyses. In the bivariate plot comparisons,

frontal breadth vs. frontal height and frontal length L vs. height were used to depict the main index changes among the groups. For the PCA, two analyses were run: one with all nine variables, and another with five variables that can be measured on the original Nanjing 1 endocast portions. These include frontal breadth, frontal height, frontal length L, height, and biasterionic breadth.

For the petalial patterns, the right side of the occipital lobe is incomplete, so it is hard to decide which side protrudes more posteriorly and/or is wider. Because the anterior portion of the Nanjing 1 endocast reflects preserved portions of the cranium, we can judge the frontal petalial patterns. The method for determining derives from LeMay et al. (1982), who scored which hemisphere protruded further rostrally (for the frontal petalia) in addition to which hemispheres were widest. Since that pioneering work, it has become clear that protrusion petalias are extremely difficult to score because they can change with the slightest rostral or caudal rotation of an endocast (Wu et al., 2006). Thus, petalias are more likely to be reliably scored by comparing widths rather than rostral/caudal projections (Zilles et al., 1996). We therefore collected width data measured at a point located 10% of the length back from the plane abutting the frontal lobes to that abutting the occipital lobes. Accordingly, Nanjing 1 manifests a left frontal petalia width pattern (Fig. 3a).

RESULTS

Morphological features

The Nanjing 1 endocast is narrow in the front and wide in the middle with an ovoid form (Fig. 2a). The maximum breadth is at the level of the superior and posterior portion of the superior temporal gyrus (Fig. 2a,c). In terms of overall cerebral height, Nanjing 1 is proportionally low when compared to its maximum length and width dimensions, and it is similar to other *H. erectus* endocasts where the widest point is usually in a low position.

The Nanjing 1 frontal region shows the usual degree of platycephaly (Fig. 2b) found in most other *H. erectus* endocasts (such as Hexian, the ZKD endocasts, and KNM-WT 15000) (Wu et al., 2010). Unlike the morphology of the ZKD specimens and Hexian, the orbital margin is round and no prominent sagittal keeling appears along the frontal lobe (Fig. 2b). The sulci and gyri impressions are well-marked on the frontal lobe of the Nanjing 1 endocast. Compared to other *H. erectus* and recent modern human endocasts, the areas of the superior frontal gyrus (Fig. 2a; also see Fig. 1c) are wide, strongly protruding and very developed. The left triangular part of the third inferior frontal gyrus (Fig. 2b) is clearly identified and shows both strong lateral and inferior protrusion similar to modern humans, although the opercular, triangular, and orbital parts cannot be fully delineated. The parietal lobes show almost no sulcal details, except for the left Sylvian fissure (lateral sulcus) that is partially and deeply etched on the left side anteriorly (Fig. 2b). The occipital lobes are wide, without any strong protuberance posteriorly (Fig. 1c). The cerebellar lobes are long, low, and quite distinct and separated at the midline. They are definitely positioned anterior to the occipital poles (Figs. 1d and 2d).

The left meningeal vessels (Fig. 2c) show a pattern typical of *H. erectus*. The anterior portions are weakly defined, and the posterior branch is clearly visible. The left frontal lobe shows weak meningeal traces. The superior sagittal sinus is visible and deviates to the left at the confluence. The transverse sinus is stronger on the left side (Fig. 2d). The venous sinus pattern is similar to modern humans as described in Wu et al. (2006).

Morphometric comparisons

Metric data for Nanjing 1 and comparative endocasts are included in Table 2. The cranial capacity of Nanjing 1, at ~876 cc, is in the low end of the range for *H. erectus* (732–1,290 cc) and it is significantly smaller than the Neanderthal (1,290–1,720 cc) and recent modern human (1,208–1,750 cc) ranges. The nine linear measurements of Nanjing 1 are all in the range of the *H. erectus* sample, and they are smaller than the Neanderthal values. Compared with the recent modern humans, Nanjing 1 has a notably lower height (49.1 mm) and frontal height (44.2 mm), a narrower frontal breadth (83.9 mm), and a shorter frontal length (66.9 mm on the left, 68.1 mm on the right). It falls within the lower end of the recent modern human ranges for length, breadth, and cerebellar breadth. The biasterionic breadth, at 97.7 mm, is close to the recent modern human mean of 98.7 mm.

Figure 4 includes bivariate plots of selected measures for Nanjing 1, other *H. erectus*, Neanderthals and recent modern humans. In the plot of frontal breadth vs. frontal height (Fig. 4a), ZKD X, ZKD XI, ZKD XII, La Ferrassie and Spy 2 cluster together with the modern humans. Nanjing 1, together with most of the other *H. erectus*

TABLE 2. The mean and ranges of cranial capacity (cc) and measurements (mm) for endocasts of Nanjing 1, Neanderthals, and modern humans

	Nanjing 1	*H. erectus* (range)	Neanderthals (range)	Modern humans (range)
Cranial capacity	876	985 (732–1,290)	1,479 (1,290–1,720)	1,423 (1,208–1,750)
Length	162.9	161.0 (143.5–178.5)	178.1 (167.0–186.5)	172.1 (153.4–192.5)
Breadth	121.5	125.3 (115.0–137.5)	143.4 (136.0–151.5)	135.3 (118.6–150.3)
Height[a]	49.1	56.0 (48.5–65.0)	64.7 (58.5–72.4)	74.3 (66.5–83.9)
Frontal breadth[a]	83.9	91.4 (80.5–103.0)	106.5 (103.0–110.9)	100.1 (87.8–113.5)
Frontal height[a]	44.2	51.2 (41.9–60.1)	57.5 (48.1–64.7)	64.3 (58.1–72.6)
Frontal length L[a]	68.1	74.4 (64.2–88.7)	81.6 (70.8–91.9)	82.8 (73.9–93.1)
Frontal length R	66.9	74.5 (64.9–86.8)	81.9 (71.7–91.8)	83.3 (74.2–93.3)
Biasterionic breadth[a]	97.7	94.0 (87.8–103.0)	105.6 (100.0–110.0)	98.7 (86.5–113.0)
Cerebellar breadth	101.5	100.1 (93.0–108.5)	111.8 (105.0–119.9)	106.8 (97.0–121.5)

[a] Measurements from original rostral and caudal endocasts.

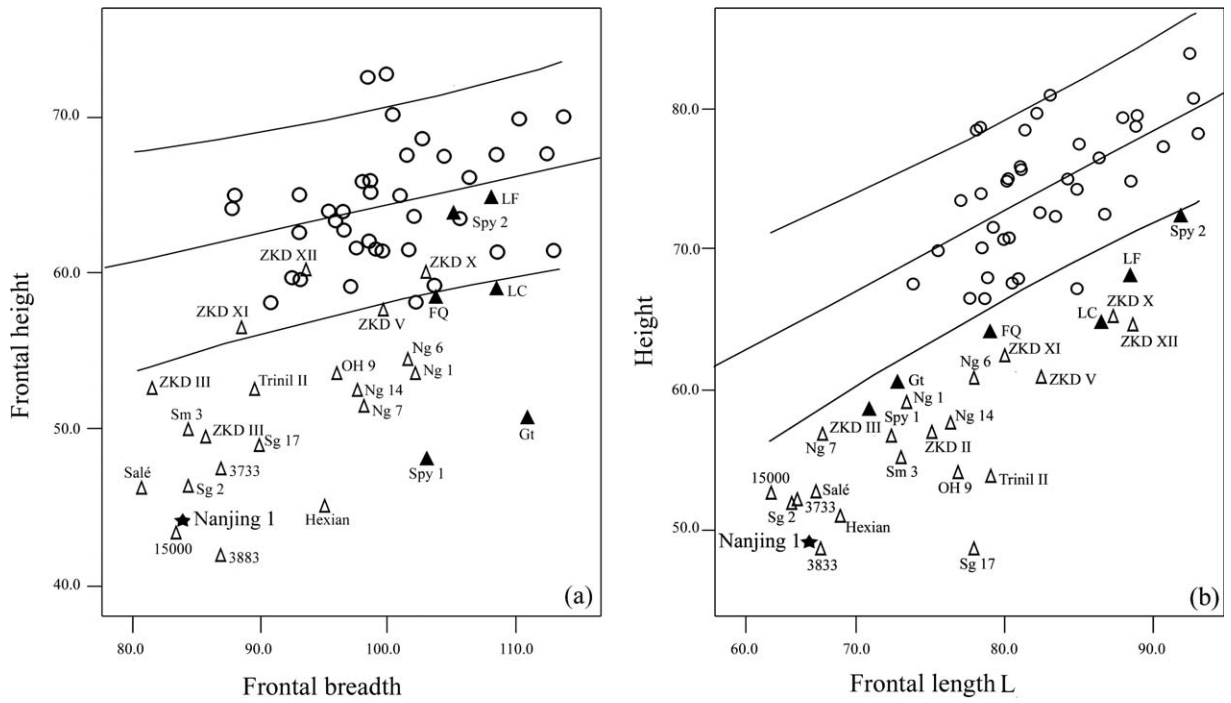

Fig. 4. Bivariate plots of endocast measures for Nanjing 1, other *H. erectus*, Neanderthals, and modern humans: (**a**) Frontal breadth vs. frontal height; (**b**) Frontal length L vs. height. Linear regression with 95% individual prediction interval is presented for the modern specimens. Circles indicate modern human specimens.

specimens, La Chapelle-aux-Saints, Spy 1, Guattari I and Forbes' Quarry, is outside the range of the linear regression with 95% individual prediction interval for the modern humans in our sample. Nanjing 1 falls closest to KNM-WT 15000, KNM-ER 3883, Salé, Sangiran 2, and Hexian. The frontal lobes of Nanjing 1 are considerably narrower and lower than most of the comparative endocasts.

According to the plot of frontal length L vs. height (Fig. 4b), Nanjing 1, together with all other *H. erectus* and Neanderthals, is beyond the range of the linear regression with 95% individual prediction interval for the modern humans in our sample. Nanjing 1 is closest to KNM-ER 3883, KNM-ER 3773, KNM-WT 15000, Salé, Sangiran 2 and Hexian, and is considerably shorter in the frontal lobes and lower in brain height than most of the other endocasts.

The PCA provide further information on the shape of Nanjing 1 and the comparative endocasts. In the nine-variable analysis (Fig. 5a), the first two components account for 85.8% of the total variance (Table 3). The first component (71.7%) is primarily related to size variation as there are positive loadings for all variables. The highest loadings are for measures of length, including the overall total length and the frontal component of length (frontal length L and frontal length R). The second component (14.7%) is mainly related to the biasterionic breadth and cerebellar breadth, although the loading for frontal height suggests it is also relatively important for describing shape variation in this sample. Based on the plot of the first two principal components (Fig. 5a), the recent modern humans cluster together with ZKD V, ZKD X, ZKD XI, ZKD XII, Ngandong 1, Ngandong 6, Ngandong 14, La Ferrassie, La Chapelle-aux-Saints, Spy 2, and Forbes' Quarry. Nanjing 1 is closest to KNM-ER 3883, Sangiran 2, Salé, KNM-ER 3733, KNM-WT 15000, and ZKD III—illustrating the overall short brain length and short frontal length components in combination with wide posterior lobes.

For the five-variable PCA (Table 3), we choose variables derived exclusively from the "original" Nanjing 1 endocast (height, frontal breadth, frontal height, frontal length L, and biasterionic breadth). The first and second principal components represent 70.1% and 16.7% of the total variance. The first component, with all positive loadings, is again related to size variation with height and frontal height making the largest contributions. The second component is mainly related to the biasterionic breadth although the frontal breadth also contributes to explaining the shape variation in the sample. Figure 5b presents the distribution of the endocasts in the subspace of the first two PCs. The modern humans cluster together with ZKD V, ZKD X, ZKD XI, ZKD XII, La Ferrassie, and Spy 2. Nanjing 1 plots closest to KNM-ER 3883, and clusters with ZKD II, ZKD III, and the Indonesian and other African *H. erectus* specimens—illustrating the combination of a low overall brain and frontal heights with wide posterior lobes. For the five-variable PCA we see the importance of height, which is clearly different for Nanjing 1 and the *H. erectus* specimens as compared to the other specimens.

DISCUSSION

This study presents the morphological and morphometrical features of the Nanjing 1 *H. erectus* endocast. Considering the ontogenetic relationship between brain shape and the interior surfaces of the cranial bones,

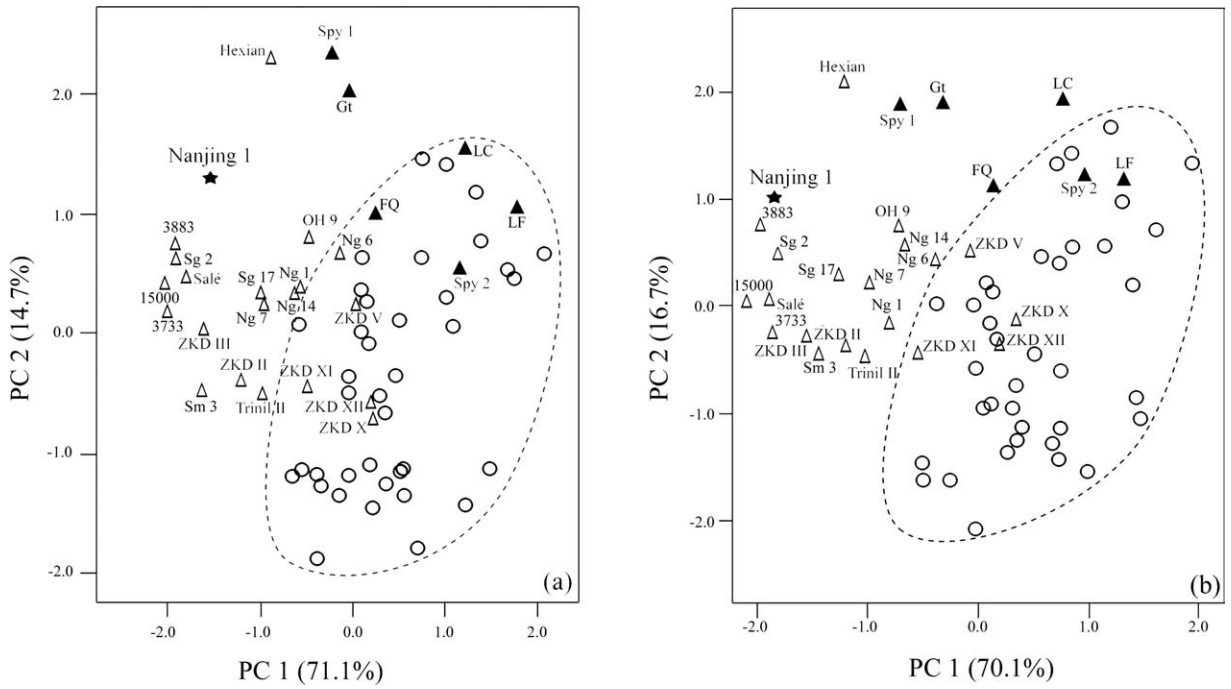

Fig. 5. Principal component analysis of Nanjing 1, other *H. erectus*, Neanderthals, and modern humans: (**a**) with all nine measurements, and (**b**) with five measurements based on landmarks represented on the original Nanjing 1 endocast reconstruction. Circles indicate modern human specimens.

TABLE 3. Principal components analysis loadings: nine-variable and five-variable analyses of Nanjing 1 and other comparative endocasts

	Nine-variable		Five-variable	
Variable	PC 1	PC 2	PC 1	PC 2
Length	0.892	0.157		
Breadth	0.853	0.337		
Height	0.835	−0.386	0.911	−0.277
Frontal breadth	0.824	0.266	0.776	0.371
Frontal height	0.856	−0.471	0.933	−0.328
Frontal length L	0.884	−0.374	0.892	−0.189
Frontal length R	0.862	−0.387		
Biasterionic breadth	0.727	0.520	0.635	0.690
Cerebellar breadth	0.845	0.431		
Percent of variance	71.1%	14.7%	70.1%	16.7%

endocasts from fossil crania provide useful information on hominin cerebral morphology and anatomy (Bookstein et al., 1999; Bruner, 2004).

The geological age of Nanjing 1 is estimated to be ~0.6 Ma, which is similar to the ages of the ZKD specimens and Sangiran 17 (Swisher et al. 1994; Shen et al., 2009) and places Nanjing 1 in the temporal range of Chinese *H. erectus*. The Nanjing 1 site lies geographically between ZKD in North China and the more southern *H. erectus* localities of Indonesia. The size of Nanjing 1, at ~876 cc, is in the lower portion of the range of endocranial volumes obtained for *H. erectus* specimens (Rightmire, 2004; also see Table 2); it has the smallest cranial capacity of the Chinese *H. erectus* group.

The Nanjing 1 endocast preserves some morphological features of taxonomic value (low overall cerebral height and low position of the greatest breadth, a flat and narrow frontal, and anterior positioning of the cerebellar lobes relative to the occipital lobes) that are generally comparable with other *H. erectus* endocasts and distinguishes them from the recent modern humans.

The frontal lobes are one of the most studied areas on fossil endocasts because of their presumed role in higher cognitive functions and language. Earlier small-brained hominins usually produce more detailed endocasts than do later larger-brained hominins (Falk, 1987). Even so, the sulci and gyri of the prefrontal lobe are clearly identifiable on the Nanjing 1 endocast (Figs. 1 and 2). Compared to the ZKD, Hexian and other *H. erectus* endocasts, Nanjing 1 has a larger, wider and more strongly swelling superior frontal sulcus in dorsal view, and the third inferior frontal areas, involving Broca's regions, show strong lateral and inferior protrusion. The superior frontal sulcus appears swollen on the LB 1 *H. floresiensis* endocast (Falk et al., 2005), but not on the other *H. erectus* endocasts, Neanderthals, or recent modern human endocasts in our sample. This strong development of the superior frontal sulcus and the other frontal lobe features is possibly a unique feature of the Nanjing 1 endocast, but more specimens are necessary to prove such a contention. It is more likely that these gyri fall well within the normal range of *H. erectus* endocasts.

The petalial patterns are frequently noted in paleontological studies because of their presumed role in laterality and handedness. In most modern humans, the petalial patterns are right frontal width and left occipital protrusion and width (LeMay, 1976; LeMay et al., 1982; Galaburda et al., 1978; Holloway and De La Coste-Lareyondie, 1982). In our study, Nanjing 1 appears to have a left frontal width petalial pattern based on the original endocast portions, but we cannot be certain

regarding the occipital and parietal lobes, and therefore cannot define a definite petalial pattern for the Nanjing 1 endocast. KNM-WT 15000, Sambungmacan 3, Hexian and ZKD III show right frontal petalial patterns, while the other ZKD endocasts show left frontal (ZKD X, ZKD XI, and ZKD XII) patterns. The petalial patterns are therefore variable in *H. erectus*. It is difficult to connect these petalial patterns with their presumed role in laterality and handedness, although their presence does document a consistent pattern of hemispheric asymmetry (Galaburda et al., 1978; Zilles et al., 1996).

The occipital lobes and cerebellar size have been hypothesized to show a steady reduction relative to cerebral size during human evolution (Holloway, 1995; Weaver, 2005). This is expressed as a change from a more posterior location (behind the parietal areas) to a more anterior location (under the parietal structures). The cerebellar lobes of Hexian, the ZKD specimens and Sambungmacan 3 are anterior to the occipital lobes, and these endocasts have strong posterior projection of the occipital lobes. This is not shown on Nanjing 1, which has no strong posterior projection of the occipital lobes. For this feature, Nanjing 1 is more similar to some of the African and the other Indonesian *H. erectus*.

Our metric data indicate that the linear measurements of the Nanjing 1 endocast are all within the range of *H. erectus*, but they fall below the range of Neanderthals. There is overlap with the lower portion of the recent modern human ranges for length, breadth, biasterionic breadth, and cerebellar breadth. These metric data support the morphological assessment that Nanjing 1 is attributable to *H. erectus*, although it is clearly among the smallest members of the taxon in terms of its estimated cranial capacity; it groups with the geologically older *H. erectus* from Africa and Indonesia (Table 1).

The bivariate plots and multivariate analysis show that Nanjing 1 is generally most similar to KNM-WT 15000, KNM-ER 3883, Salé, Sangiran 2, and Hexian in displaying narrow, low, and short frontal lobes and wide posterior lobes. Compared with all of the *H. erectus* in our sample, the shape of Nanjing 1 is furthest from the ZKD endocasts. This lends support to the notion of a gradient in morphology running north to south in East Asia (Wolpoff, 1985; Zhang and Liu, 2007). The differences among Nanjing 1, Hexian, and the ZKD specimens suggest that there is also a certain level of regional variation in East Asian *H. erectus* (Zhang and Liu, 2005).

CONCLUSIONS

Overall, the Nanjing 1 endocast shares some common morphological and morphometric features with other *H. erectus* endocasts that distinguish them from the Neanderthals and modern humans: the cranial capacity is small, the widest point on the endocast is located low on the parietal lobes, the shape is ovoid in superior view, the frontal region is shorter and flattened, the cerebral height is low, the cerebellar lobes are distinct and do not meet in the midline, and the middle meningeal vessel patterns are relatively simple. When we compared Nanjing 1 with the ZKD individuals, Hexian, and the Indonesian and African *H. erectus* specimens, Nanjing 1 has unique, large, superior frontal convolutions, and lacks strong posterior projection of the occipital lobes. The morphometric analysis show that the Nanjing 1 is more similar to some of the geologically earlier African and Indonesian *H. erectus* than it is to the other Chinese specimens. This is an interesting result that illustrates the metrical diversity of Asian *H. erectus*; it is not unexpected given the temporal and geographical range of the species. The Nanjing 1 endocast is an important addition to our understanding of the variability of *H. erectus* endocast remains in China and elsewhere.

ACKNOWLEDGMENTS

The authors thank Zhang Yinyun and Liu Wu for their help in preparing the endocast of Nanjing 1 and their useful suggestions and encouragement. They are grateful for the helpful comments of anonymous reviewers on an earlier version of this manuscript.

LITERATURE CITED

Balzeau A, Grimaud-Hervé D, Jacob T. 2005. Internal cranial features of the Modjokerto child endocranium (East Java, Indonesia). J Hum Evol 48:535–553.

Begun D, Walker A. 1993. The endocast. In: Walker A, Leakey R, editors. The Nariokotome *Homo erectus* skeleton. Cambridge: Harvard University Press. p 326–358.

Black D. 1933. On the endocranial cast of the adolescent *Sinanthropus* skull. Proc R Soc B 112:263–276.

Bookstein F, Schäfer K, Prossinger H, Seidier H, Fieder M, Stringer C, Weber GW, Arsuaga J, Slice DE, Rohlf FJ, Recheis W, Mariam AJ, Marcu LS. 1999. Comparing frontal cranial profiles in archaic and modern *Homo* by morphometric analysis. Anat Rec 257:217–224.

Broadfield DC, Holloway RL, Mowbray K, Silvers A, Yuan MS, Marquez S. 2001. Endocast of Sambungmacan 3 (Sm 3): a new *Homo erectus* from Indonesia. Anat Rec 262:369–379.

Brown FH, Harris J, Leakey R, Walker A. 1985. Early *Homo erectus* skeleton from west Lake Turkana, Kenya. Nature 316:788–792.

Brown FH, McDougall I. 1993. Geologic setting and age. In: Walker A, Leakey R, editors. The Nariokotome *Homo erectus* skeleton. Cambridge: Harvard University Press. p 9–20.

Bruner E. 2003. Fossil traces of the human thought: paleoneurology and the evolution of the genus *Homo*. Rivista di Antropologia 81:29–56.

Bruner E. 2004. Geometric morphometrics and paleoneurology: brain shape evolution in the genus *Homo*. J Hum Evol 47:279–303.

Bruner E, Manz G. 2005. CT-based description and phyletic evaluation of the archaic human calvarium from Ceprano, Italy. Anat Rec 285A:643–658.

Chen T, Wu E, Yang Q, Hu Y. 1997. The ESR dating of the Nanjing *Homo erectus* stratigraphy. Nucl Tech 20:732–734.

Delson E, Harvati K, Reddy D, Marcus LF, Mowbray K, Sawyer GJ, Jacob T, Márquez S. 2001. The Sambungmacan 3 *Homo erectus* calvaria: a comparative morphometric and morphological analysis. Anat Rec 262:380–397.

Dubois E. 1933. The shape and size of the brain in *Sinanthropus* and in *Pithecanthropus*. Proc Acad Sci Amsterdam 36:1–9.

Falk D. 1987. Hominid paleoneurology. Ann Rev Anthropol 16:13–30.

Falk D. 1993. Meningeal arterial patterns in great apes: implications for hominid vascular evolution. Am J Phys Anthropol 92:81–97.

Falk D, Hildebolt C, Smith K, Morwood MJ, Sutikna T, Brown P, Jatmiko, Saptomo EW, Brunsden B, Prior F. 2005. The brain of LB1, *Homo floresiensis*. Science 8:242–245.

Galaburda AM, LeMay M, Kemper TL, Geschwind N. 1978. Right-left asymmetries in the brain. Science 199:852–856.

Grimaud-Hervé D. 1997. L'évolution de l'enchéphale chez *Homo erectus* et *Homo sapiens*. Paris: CNRS Editions.

Grimaud-Hervé D. 2004. Meningeal patterns. In: Holloway RL, Broadfield DC, Yuan MS, editors. The human fossil record, Vol. 3: Brain endocasts—the paleoneurological evidence. New York: Wiley-Liss. p 273–282.

Grün R, Huang PH, Huang WP, McDermott F, Thorne A, Stringer CB, Yan G. 1998. ESR and U-series analyses of teeth from the palaeoanthropological site of Hexian, Anhui Province, China. J Hum Evol 34:555–564.

Holloway RL. 1980. Indonesian "Solo" (Ngandong) endocranial reconstructions: some preliminary observations with Neanderthal and *Homo erectus* groups. Am J Phys Anthropol 53:285–295.

Holloway RL. 1981. The Indonesian *Homo erectus* brain endocasts revisited. Am J Phys Anthropol 55:503–521.

Holloway RL. 1995. Toward a synthetic theory of human brain evolution. In: Chaneaux JP, Chavaillon J, editors. Origins of the human brain. Oxford: Clarendon. p 42–54.

Holloway RL, Broadfield DC, Yuan MS. 2004. The human fossil record, Vol. 3: Brain endocasts—the paleoneurological evidence. New York: Wiley-Liss.

Holloway RL, De La Coste-Lareymondie MC. 1982. Brain endocast asymmetry in pongids and hominids: some preliminary findings on the paleontology of cerebral dominance. Am J Phys Anthropol 58:101–110.

LeMay M. 1976. Morphological cerebral asymmetries of modern man, and nonhuman primates. Ann N Y Acad Sci 280:349–366.

LeMay M, Billing MS, Geschwind N. 1982. Asymmetries of the brains and skulls. In: Armstrong E, Falk D, editors. Primate brain evolution. New York: Plenum. p 263–277.

Liu W, Zhang Y, Wu X. 2005. A middle Pleistocene human cranium from Tangshan, Nanjing of southeast China: a comparison with *Homo erectus* from Eurasia and Africa based on new reconstruction. Am J Phys Anthropol 25:253–262.

Qiu ZL, Gu YM, Zhang YY, Zhang SS. 1973. Newly discovered *Sinanthropus* remains and stone artifacts at Zhoukoudian. Vertebr Palasiatica 11:109–131.

Rightmire GP. 2004. Brain size and encephalization in early to mid-Pleistocene *Homo*. Am J Phys Anthropol 124:109–123.

Shang H, Trinkaus E. 2008. An ectocranial lesion on the middle Pleistocene human cranium from Hulu cave, Nanjing, China. Am J Phys Anthropol 135:431–437.

Shen G, Gao X, Gao B, Granger D. 2009. Age of Zhoukoudian *Homo erectus* determined with $^{26}Al/^{10}Be$ burial dating. Nature 458:198–200.

Sholts SB, Flores L, Walker PL, Wärmländer SKTS. Comparison of coordinate measurement precision of different landmark types on human crania using a 3D laser scanner and a 3D digitiser: implications for applications of digital morphometrics. Int J Osteoarchaeol, in press (Article first published online: 22 Feb 2010, DOI: 10.1002/oa.1156).

Swisher CC III, Curtis GH, Jacob J, Getty AG, Suprijo A, Widiasmoro. 1994. Age of the earliest known hominids in Java, Indonesia. Science 263:1118–1121.

Tangshan Archaeological Team from Nanjing Municipal Museum and Archaeology Department of Peking University. 1996. Locality of the Nanjing man fossils. Beijing: Cultural Relics Publishing House.

Weaver AH. 2005. Reciprocal evolution of the cerebellum and neocortex in fossil humans. Proc Natl Acad Sci USA 102:3576–3580.

Weidenreich F. 1936. Observations on the form and proportions of the endocranial casts of *Sinanthropus pekinensis*, other hominids and the great apes: a comparative study of brain size. Paleontol Sin NSD 7:1–50.

Weidenreich F. 1939. The phylogenetic development of the hominid brain and its connection with the transformation of the skull. Bull Geol Soc China 19:28–46.

Weidenreich F. 1943. The skull of *Sinanthropus pekinensis*: a comparative study on a primitive hominid skull. Paleontol Sin NS 10:108–113.

Wolpoff MH. 1985. Human evolution at the peripheries: the pattern at the eastern edge. In: Tobias PV, editor. Hominid evolution: past, present and future. In Proceedings of the Taung Diamond Jubilee International Symposium, Johannesburg and Mmabatho, South Africa, 27th January-4th February. New York: Alan R Liss. p 355–365.

Wu R, Zhang Y, Wu X. 2002. Nanjing skull No. 1. In: Wu R, Li X, Wu X, Mu X, editors. Homo erectus from Nanjing. Nanjing: Jiangsu Science and Technology Publishing House. p 261–273.

Wu RK, Dong XR. 1982. Preliminary study of *Homo erectus* remains from Hexian, Anhui. Acta Anthrop Sin 1:2–13.

Wu XJ, Schepartz L, Falk D, Liu W. 2006. Endocast of Hexian *Homo erectus* from south China. Am J Phys Anthropol 130:445–454.

Wu XJ, Schepartz LA, Liu W. 2010. Endocranial cast of Zhoukoudian Skull V: a new *Homo erectus* brain endocast from China. Proc R Soc B 277:337–344.

Zhang Y, Liu W. 2002. The reconstruction of *Homo erectus* cranium from Tangshan, Nanjing, and the geographic variation of *Homo erectus* in Middle Pleistocene. Earth Sci Frontiers 9:119–123.

Zhang Y, Liu W. 2003. Cranial capacity estimation for *Homo erectus* from Tangshan, Nanjing. Acta Anthrop Sin 22:201–205.

Zhang Y, Liu W. 2005. Comparison of *Homo erectus* from Nanjing with those from Zhoukoudian and Sangiran in facial morphology. Acta Anthrop Sin 24:171–177.

Zhang Y, Liu W. 2007. A morphological comparison of two *Homo erectus* crania: Nanjing 1 and KNM-ER3733. Acta Anthrop Sin 26:237–248.

Zhao J, Hu K, Collerso K, Xu H. 2001. Thermal ionization mass spectrometry U-series dating of a hominid site near Nanjing, China. Geology 29:27–30.

Zhou C, Wang Y, Cheng H, Liu Z. 1999. Discussion on Nanjing man's age. Acta Anthrop Sin 18:255–262.

Zilles K, Dabringhaus A, Geyer S, Amunts K, Qü M, Schleicher A, Gilissen E, Schlaug G, Steinmetz H. 1996. Structural asymmetries in the human forebrain and the forebrain of non-human primates and rats. Neurosci Biobehav Rev 20:593–605.

Zollikofer CP, Ponce de Leon M. 2005. Virtual reconstruction: a review in computer-assisted paleontology and biomedicine. New York: Wiley-Liss.